Electron Tunneling Through Thin Aluminum Oxide Films*

THOMAS E. HARTMAN AND JAY S. CHIVIAN
Texas Instruments Incorporated, Dallas, Texas
(Received 13 December 1963)

The thin-film Al-Al_2O_3-Al system is studied. The current density as a function of temperature and voltage through aluminum oxide less than 30 Å thick is analyzed using the theory of Stratton. The charge transport mechanism is established as tunneling by the functional form of the small temperature dependence. By fitting the current density data to the temperature dependence for $79°K < T < 300°K$ and $0 \leq V \leq 1.0$ V, the integrals arising from the WKB approximation are evaluated for an arbitrary barrier shape. The region of applied voltage for which quadratic power series expansions in V of these integrals are valid is established as $0.0 \leq V \leq 0.3$ V. Assuming a trapezoidal barrier shape, approximate values for the barrier heights of 0.89 and 0.78 eV and an electron effective mass of $m^*/m = 1$ are deduced. Comparisons are drawn between the more general forms of Stratton's and Simmons' theories.

I. INTRODUCTION

THE flow of electrons through a sufficiently thin insulating film will occur by the quantum mechanical mechanism of tunneling.[1] Barrier layers thicker than a few tens of angstroms are nearly impenetrable to tunneling electrons, as the transmission probability falls off exponentially with thickness, except where the tunnel distance is shortened by the application of a sufficiently large voltage (i.e., Fowler-Nordheim[2,3] region). For diminishingly small applied voltages, the electronic conductivity of films a few tens of angstroms thick may arise from thermionic or Schottky emission over the barrier,[4] tunneling through the barrier, space-charge limited current,[5] or a combination of these mechanisms with traps in the forbidden gap of the insulator participating as an intermediary.[6]

At temperautres below the superconducting transition for the aluminum films in the Al-Al_2O_3-Al system, the electron current through an aluminum oxide film a few tens of angstroms thick has been shown to result from tunneling.[7] The thermionic or Schottky contribution to the current is clearly negligible at these temperatures.

Emtage and Tantraporn[4] have reported that for the Al-Al_2O_3-Al system the entire current through a 50-Å-thick oxide film at room temperature appears to come from Schottky emission. Whether thermionic emission or tunneling dominates the zero-voltage conductivity depends very strongly on the thickness of the oxide film. For sufficiently thin oxide films tunneling will be the dominant conduction mechanism. It is easy to show for the Al-Al_2O_3-Al system, assuming a rectangular barrier 0.85 eV high and an effective mass $m^*/m = 1$, that at room temperature the critical thickness is 35 Å (or thinner), tunneling will dominate almost exclusively. For oxide films thicker than 35 Å, thermionic or Schottky emision will dominate and the conductivity will be highly temperature-dependent.

The current density through aluminum oxide films less than 30 Å thick, sandwiched between two aluminum films, was measured as a function of temperature and voltage. The conduction mechanism, even for diminishingly small applied voltages, is shown to be tunneling by the functional form of relatively small temperature dependence. The data are analyzed using the theory of Stratton.[8] Using the barrier height and thickness deduced from the data the Schottky current was calculated and found to be more than two orders of magnitude less than the measured current at room temperature. The integrals arising from the WKB approximation in the theory are evaluated for an arbitrary potential barrier shape by fitting the current density data to the temperature dependence. Finally, the theory of Stratton is modified to take more accurate account of the back current, which is the current that flows in the direction opposite to the current which is aided by the applied potential. The resulting equation can be reduced to either Stratton's or Simmons' theory depending on the approximations employed.

II. EXPERIMENTAL TECHNIQUE

A. Sample Preparation

The configuration of the aluminum-aluminum oxide-aluminum thin-film sandwiches employed in these experiments is shown schematically in Fig. 1. The substrate is a glass microscope slide cleaned by a technique similar to that of Lowe.[9] The slide is subsequently ion bombarded in the manner described by Holland.[10]

The metal layers are deposited on an unheated substrate in a vacuum-evaporation system at a pressure of less than 1×10^{-6} Torr. The composition of the resi-

* Presented in part at the Pasadena meeting of the American Physical Society, December 1963.

[1] R. Holm, *Electric Contacts* (Hugo Gerer, Stockholm, Sweden, 1946).

[2] R. Fowler and L. Nordheim, Proc. Roy. Soc. (London) **A119**, 173 (1928).

[3] C. A. Mead, J. Appl. Phys. **32**, 646 (1961).

[4] P. R. Emtage and W. Tantraporn, Phys. Rev. Letters **8**, 267 (1962).

[5] D. V. Geppert, J. Appl. Phys. **33**, 2993 (1962).

[6] C. A. Mead, Phys. Rev. **128**, 2088 (1962).

[7] I. Giaever and K. Megerle, Phys. Rev. **122**, 1101 (1961).

[8] R. Stratton, Phys. Chem. Solids **23**, 1177 (1962).

[9] L. Holland, *Vacuum Deposition of Thin Films* (J. Wiley & Sons Inc., New York, 1958), p. 71.

[10] L. Holland, *Vacuum Deposition of Thin Films* (J. Wiley & Sons Inc., New York, 1958), p. 84.

TABLE I. Residual gas analysis.[a]

Gas or vapor	Partial pressure, % of total pressure
Water vapor	89
Carbon monoxide	8
Nitrogen	1
Oxygen	1
dc 704 (pump oil)	<1

[a] The residual gas analysis was made with a mass-spectrometer similar to the one described by W. D. Davis and T. A. Vanderslice, *Vacuum Symposium Transactions*, edited by C. R. Meissner (Pergamon Press, Inc., London, 1960), p. 417.

dual gasses in the system at its ultimate pressure of 3×10^{-8} Torr are shown in Table I. The silver used for contacts and interferometry gauges is vaporized from a molybdenum Knudsen surface emitting source[11] and the 99.999+% pure aluminum is vaporized from a tungsten hairpin filament source.[12]

First the lower aluminum layer is deposited on aluminum contacts. The slide is then removed from the vacuum system, and placed in a preheated furnace of dry air at atmospheric pressure and a temperature of 300°C for two to four hours.[13] The slide is then vapor degreased in isopropyl alcohol, replaced in the vacuum system, ion bombarded, and the remaining metal layers are deposited.

The metal films are each approximately 1000 Å thick. The junction area is 10^{-2} cm^2, and is coated with a protective layer of silicon monoxide 2000 to 3000 Å thick (not shown in Fig. 1) using a tantalum perforated chimney source similar to the one described by Drumheller.[14] The samples are stored in a vacuum desiccator at room temperature.

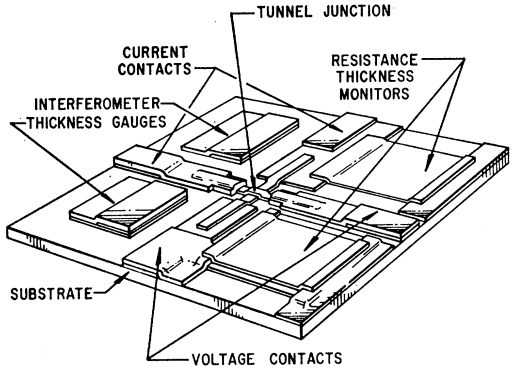

FIG. 1. Sample configuration.

[11] L. Holland, *Vacuum Deposition of Thin Films* (John Wiley & Sons, Inc., New York, 1958), p. 119.

[12] S. Dushman, *Scientific Foundations of Vacuum Technique*, edited by J. M. Lafferty (John Wiley & Sons, Inc., New York, 1962), p. 706.

[13] The rate of oxidation of evaporated aluminum films in very dry atmospheres of air or oxygen is observed to be much slower than when water vapor is present in small quantities in agreement with the results of P. E. Blackburn and E. A. Gulbransen, J. Electrochem. Soc. **107**, 944 (1960) and I. Giaever and K. Megerle, Phys. Rev. **122**, 1101 (1961).

[14] C. E. Drumheller, *Vacuum Symposium Transactions*, edited by L. E. Preuss (Pergamon Press, Inc., London, 1961), p. 306.

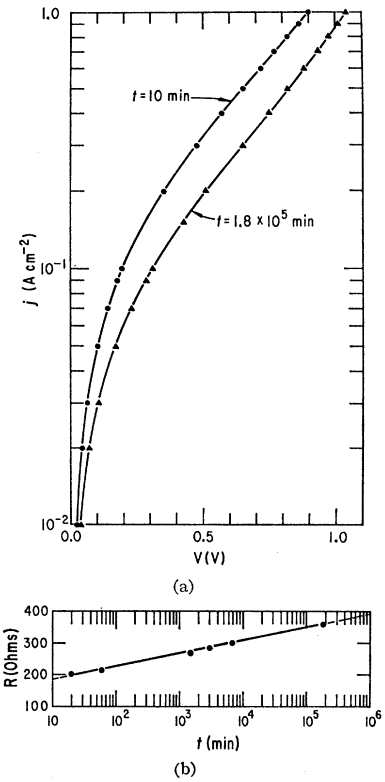

FIG. 2. Electrical characteristics of a typical sample as a function of time. (a) Initial and final plot of the current density as a function of the applied voltage. (b) Plot of the zero bias junction resistance as a function of time.

B. Sample Characteristics

For applied voltages less than 90 mV, the electrical characteristics of the samples are Ohmic (see Fig. 7). The resistance and capacitance of the samples are measured using a low-frequency-transformer ratio arm bridge which impresses 90 mV rms (or less) upon the sample, hence the values obtained correspond essentially to the zero-applied-voltage condition. All other electrical measurements are made using four-terminal methods, so that lead and contact resistance errors are avoided. The resistance of the samples range from 100 to 400 ohms and their capacitance is about 0.022 to 0.028 μF. The zero-applied-voltage resistance R and the j versus V characteristics for a typical sample are shown in Fig. 2, where j is the current density, V is the applied voltage, and t is the time ($t=0$ is the time when the sample fabrication was completed).

An increase in the junction resistance of the same general form as that reported by Handy[15] is observed. As shown in Fig. 2(b) the junction resistance increases approximately as the logarithm of the time. Extrapolating this plot the junction resistance would be expected to be double its initial (i.e., $t=20$ min) value at $t=1.6\times10^6$ min (or in about three years). The slope of the junction resistance versus log t is similar to that reported by Handy for unprotected junctions within 2 to 3 min after deposition of the second aluminum layer. Handy

[15] R. M. Handy, Phys. Rev. **126**, 1968 (1962).

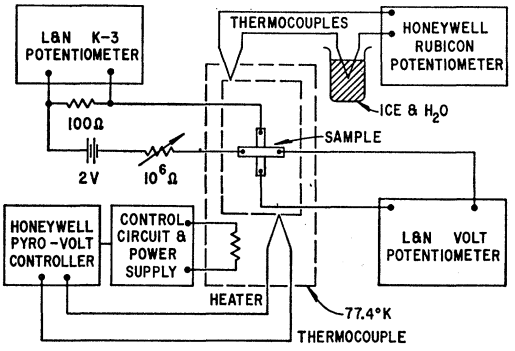

FIG. 3. Schematic diagram of electrical measurement and temperature controlling apparatus.

reported that the slope is pressure sensitive and in a vacuum of 5×10^{-2} Torr the resistance doubled in less than 3000 min (i.e., approximately two days). These results suggest that coating the junction with silicon monoxide immediately after its formation tends to preserve the initial junction characteristics.[16]

The measurement techniques described below are designed to yield 0.1% precision, which is required for the analysis of the data in the following section. The stability of the junction is consequently of prime importance. After the sample has been aged for four months the junction resistance changes 0.1% in about 3000 min which is approximately the time required to take the data for the volt-current characteristics analyzed in Sec. IV.

The change in the zero-applied-voltage resistance is accompanied by a shift in the volt-current characteristics. After storing the samples for four months, the electrical characteristics up to 1.0 V are quite stable with time. The initial plot of log j versus V and the plot after aging for four months are shown in Fig. 2(a). The final plot is reproducible to within 0.1% at a constant temperature even when the sample has been cycled to liquid-nitrogen temperature between measurements. No shorting,[17] hysteresis,[17] long time constant,[17] forming,[18,19] negative dynamic resistance,[18,20] or change in the direction or rectification with temperature[15] effects were observed. A small rectification effect is observed and is discussed in Sec. IV.

Aluminum oxide films formed by a number of different techniques have been investigated in this laboratory. Only the oxides grown thermally, as described above, were used in the experiments reported here. However, the results are considered to apply to almost all aluminum oxide films of less than 30 Å thickness grown on the surface of vacuum deposited aluminum films, provided the applied voltage is less than 0.2 V. The shape of the log j versus V plot can be correlated with the oxidation technique.[21] However, the characteristic shapes for each oxidation technique are nearly identical for applied voltage less than 0.2 V, aside from a multiplicative constant which arises from small differences in the oxide film thickness.

C. Measurement Techniques

A schematic diagram of the electrical measurement and temperature controlling apparatus is shown in Fig. 3. The apparatus is designed to maintain the sample inside a temperature-controlled light-tight chamber at any temperature between the boiling point of liquid nitrogen and room temperature. Since the substrate is a relatively poor heat conductor, it is necessary to enclose the sample in a constant temperature chamber, because the sample tends to come to radiation equilibrium with the temperature of its surroundings. The apparatus is similar to that of Ure[22] with the addition of a proportional temperature controller which regulates the dc heater power. With this apparatus the temperature can be maintained within ±0.2°K during the time required to measure the volt-current characteristics. The controlled temperature is measured with a copper-constantan thermocouple.

The dc volt-current characteristics at constant temperature are measured by setting a predetermined voltage across the junction, as compared with a volt potentiometer, and measuring the voltage drop across a 100 ohm ($\pm0.05\%$) resistance in series with the sample with a K-3 potentiometer to determine the current.

III. THEORY

The net current density j in the direction normal to the insulating film in a metal-insulator-metal system, from a conducting region 1 to a conducting region 2, through the potential barrier formed by the forbidden energy gap of the insulator, is given by Stratton's[8] general equation

$$j=\frac{4\pi mq}{c_1^2h^3}\left[\frac{\pi c_1kT}{\sin(\pi c_1kT)}\right]\exp(-b_1)[1-\exp(-c_1qV)], \quad (1)$$

where

$$b_1=\alpha\int_{x_{11}}^{x_{21}}(\varphi-\zeta_1)^{1/2}dx; \quad c_1=\frac{\alpha}{2}\int_{x_{11}}^{x_{21}}(\varphi-\zeta_1)^{-1/2}dx,$$

which are functions of the applied voltage V that arise

[16] This result is in disagreement with the results of J. Penley, J. Appl. Phys. 33, 1623 (1962), but suggests that the pressure sensitive resistance change may be due to diffusion through the unprotected top metal layer, see J. J. Wortman and R. M. Burger, Second Annual Symposium on the Physics of Failure in Electronics, 1963 (unpublished).

[17] D. Meyerhoffer and S. A. Ochs, J. Appl. Phys. 34, 2535 (1963).

[18] T. W. Hickmott, J. Appl. Phys. 33, 2669 (1962).

[19] S. R. Pollack, J. Appl. Phys. 34, 877 (1963).

[20] H. Kanter and W. A. Feibelman, J. Appl. Phys. 33, 3580 (1962).

[21] The correlation of the shape of the log j versus V curves with the oxidation technique is the subject of another paper by one of the authors (T.E.H.) (to be published).

[22] R. W. Ure, Jr., Rev. Sci. Instr. 28, 836 (1957).

from the WKB approximation and can be computed for a given barrier $\varphi(x,V)$. The limits x_{11} and x_{21} are the classical turning points given by the values of x for which $\varphi(x,V)=\zeta_1$, ζ is the Fermi energy, x is the direction normal to the insulating film, q is the charge and m the mass of the electron, h is Planck's constant, T is the absolute temperature and $\alpha=4\pi(2m)^{1/2}/h$.

Equation (1) is derived assuming a parabolic energy-momentum relation with the same electron mass in each of the three regions. Stratton[8] has shown that the equation is still valid when the effective mass in the insulator is less than the mass in either conducting region. It is found that the more general form of Stratton's equation for a nonparabolic energy-momentum relation in the insulator is not required to explain the results in Sec. IV. This presumably arises because the barrier heights deduced in Sec. IV are a small fraction of the energy gap. Other conditions on the range of application of Eq. (1) are discussed by Stratton.

The last term in brackets in Eq. (1) represents the back current, or electrons tunneling from the conducting region 2 to conducting region 1 against the applied electric field. This term diminishes in importance rapidly with increasing applied voltage. The voltage dependence of the forward current results predominantly from $b_1(V)$ in the exponential.

In deriving the equation it is assumed that the current is largely due to electrons whose energies are close to the Fermi energy in the conducting region 1. As a result an expansion with respect to energy near ζ_1 is employed. The result of this procedure is to assume that most of the current is forward current, and that even the back current arises from electrons whose energies are close to ζ_1. This is a very good approximation for all but the very small applied voltages.

The back current is more accurately represented by an expansion about the Fermi energy in the conducting region 2 given by $\zeta_2=\zeta_1-qV$.[23] From the symmetry it follows that the current density is more accurately given by

$$j=\frac{4\pi mq}{h^3}\left\{\frac{e^{-b_1}}{c_1^2}\left[\frac{\pi c_1 kT}{\sin(\pi c_1 kT)}\right]-\frac{e^{-b_2}}{c_2^2}\left[\frac{\pi c_2 kT}{\sin(\pi c_2 kT)}\right]\right\}. \quad (2)$$

From this more accurate expression both Stratton's and Simmons'[24] expressions for the current density, assuming an arbitrary barrier shape $\varphi(x,V)$, can be derived depending on the particular assumptions employed.[25] Both Eq. (2) and Simmons'[24] Eq. (20) are intractable to experimental analysis.

The difficulty in arriving at any straightforward solution for the current density, where an arbitrary (or unknown) barrier shape $\varphi(x,V)$ is involved, is the evaluation of the integrals arising from the WKB approximation. Stratton expands the functions around energies near the Fermi level to avoid the difficulty, whereas Simmons employs an approximate value for the integrals.

The advantage of Stratton's theory is that it holds for nonzero temperatures and in the form given in Eq. (1) it is tractable to experimental analysis. The unknown functions $b_1(V)$ and $c_1(V)$ can be deduced by fitting the experimental current-density data, as functions of temperature and voltage, to Eq. (1) as shown in the following section. The disadvantage is the inaccuracy in the back current, which is not serious as will be indicated.

The disadvantages to Simmons' theory are the restriction to absolute zero temperature and the experimental intractability. The advantage is that since electrons of all energies are taken into account the back current is more accurate. By combining the two approaches, some of the advantages of both can be retained. In particular, the average barrier height as defined by Simmons and the tunnel path length can be given by

$$\bar{\varphi}-\zeta_1=b_1/(2c_1), \quad (3)$$

and

$$(\Delta x)^2=2b_1c_1/\alpha^2, \quad (4)$$

respectively, in terms of Stratton's functions which can be deduced from experiment.

Finally, it is easy to show from Eq. (2) (using the values of the functions b_1 and c_1 deduced in the following section) that at a given temperature the current does not rise as rapidly with increasing voltage as implied by Eq. (1). The error decreases monotonically with increasing voltage and at 0.10 V the correction attenuates the tunnel current only about 3%. For diminishingly small applied voltages Simmons' and Stratton's expressions (at $T=0$) are equivalent. At a constant voltage, the current is less than that predicted by Eq. (1). The error decreases monotonically from a maximum of about 2% to about 1% at room temperature. The corrections to Eq. (1) stemming from the more accurate account of the back current are seen to be small.

IV. EXPERIMENTAL RESULTS

A. Temperature Dependence

It will now be shown that the experimental current density data as a function of temperature and voltage can be fitted to the functional form of the temperature dependence in Eq. (1). The temperature dependence is given by

$$j(T)\propto[\pi c_1 kT/\sin(\pi c_1 kT)]. \quad (5)$$

The functional form of Eq. (5) arises from the Fermi distribution of electrons in the metal layers and will not fit unless the electrons tunnel directly from the metal on one side to the metal on the other side (since voltages

[23] The authors are indebted to R. Stratton for pointing out this correction to the theory.

[24] J. G. Simmons, J. Appl. Phys. 34, 1793 (1963).

[25] In deriving Simmons' (Ref. 24) Eq. (20) some differences in the β factors from those of Simmons arise; however, in practice $\beta\approx 1$ over the range of interest.

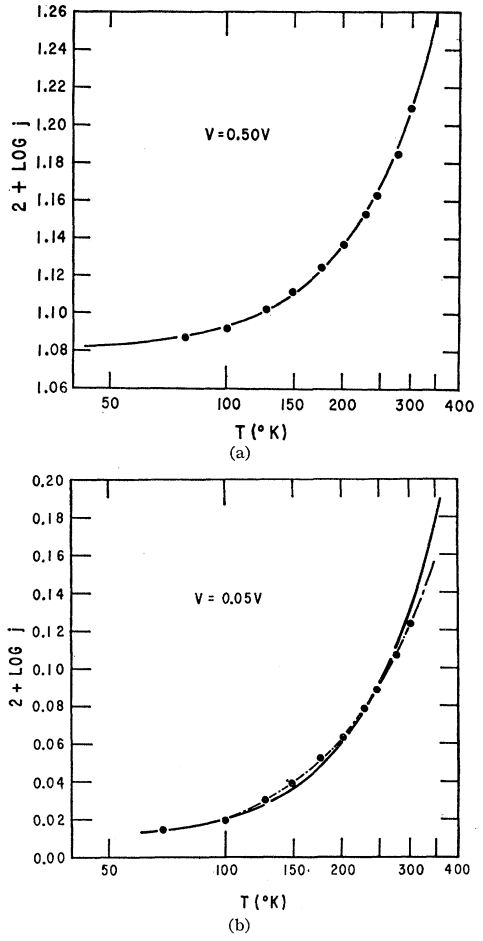

FIG. 4. The dependence of the current density on the temperature at (a) 0.50 V and (b) 0.05 V. The points are experimental data, and the curve, which is theoretical, corresponds to Eq. (1) [or the expression in (5)].

less than those required for Fowler-Nordhiem emission are employed).

The coefficients b_1 and c_1 are determined, at any particular voltage, by fitting the experimental plot of $\log_{10} j(T)$ versus $\log_{10} T$ to the theoretical plot of Eq. (5) which is $\log_{10}[\pi c_1 kT/\sin(\pi c_1 kT)]$ versus $\log_{10}(\pi c_1 kT)$. A typical example is shown in Fig. (4a). The value of c_1 is deduced from the temperature corresponding to $\pi c_1 kT=1$. Using Eq. (1), b_1 can be calculated from $j(0)$, which is deduced from the current density extraploated to absolute zero temperature corresponding to $[\pi c_1 kT/\sin(\pi c_1 kT)]=1$. The quality of the fit shown in Fig. 4(a) for 0.50 V applied potential is characteristic for all voltages between 0.10 and 0.90 V. It should be noted that the scale of the ordinate axis has been expanded greatly compared to the abscissa in order that the relatively small (e.g., compared to Schottky) temperature dependence (between 30 to 50% change in going from liquid nitrogen to room temperature) can be compared accurately with the theoretical form.

The quality of the fit of the experimental current-density data, as functions of temperature and voltage, to the functional form of the theoretical temperature dependence establishes that tunneling directly between the two aluminum layers is the predominant mechanism for the electronic conduction through the aluminum oxide film.

A typical example of the fit of the data to the expression (5) for $V<0.10$ V is shown in Fig. 4(b). The deviations may arise from small thermal emf's which can produce internal voltages, but do not appear to be due to the back current [i.e., fit the transcendental temperature dependence given in Eq. (2)]. The form of the experimental curve, shown as the dashed curve in Fig. 4(b), is characteristic of all the samples investigated at very small applied voltages.

The temperature dependence in Eq. (1) can be expanded for small temperatures in a binomial series with respect to $\pi c_1 kT$ which gives[8]

$$\Delta j = j(T)-j(0)=\frac{j(0)}{6}(\pi c_1 kT)^2 + \frac{7j(0)}{360}(\pi c_1 kT)^4+\cdots. \quad (6)$$

Chow[26] has analyzed the temperature dependence of the current density in the Be-BeO-Au system by fitting the data to the quadratic dependence given in Eq. (6) and neglecting the higher order terms. The $j(0)$ was calculated, assuming the quadratic dependence, using two of the data points. The result of plotting $\log_{10}\Delta j=\log_{10}[j(T)-j(0)]$ versus $\log_{10} T$ is a straight line of slope 2.04 up to 300°K. Similar results for the Al-Al_2O_3-Al system have also be reported.[17] Analyzing the temperature dependence data in this way is subject

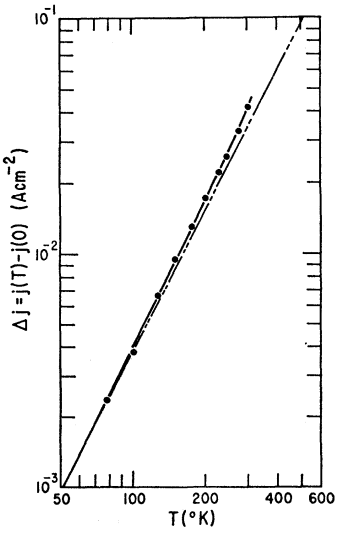

FIG. 5. The dependence of the change in the current density at 0.50 V on the temperature. The points are experimental data, the dashed line is the T^2 approximation, and the curve, which is theoretical, corresponds to Eq. (6) and includes the T^4 term.

[26] C. K. Chow, J. Appl. Phys. 34, 2919 (1963).

to considerable error. In order that the quadratic approximation hold, $j(0)$ must be determined from the data over a small range of temperatures usually between 78 and 150°K. This may result in some inaccuracy in $j(0)$ and considerable deviation of $\Delta j(T)$ from the T^2 line over the range of temperatures where the T^2 approximation is valid (cf. Chow's[26] Fig. 1). However, $j(0)$ can be determined with good accuracy using the technique described above. Using the $j(0)$ determined from Fig. 4(a), a plot of $\log_{10}\Delta j$ versus $\log_{10}T$ is shown in Fig. 5 for the experimental data shown in Fig. 4(a). Results quite similar to those of Chow are obtained except that good agreement with the T^2 linear approximation (shown as the dashed line in Fig. 5) is obtained for temperatures less than 100°K. The solid curve is a plot of the theoretical temperature dependence as given by Eq. (6) including the T^4 term, using the value of $c_1=16.0$ eV^{-1} determined from Fig. 4(a). A straight line of slope slightly greater than two can be fitted to the data in Fig. 5, but in fact it is seen that the deviation of the experimental data from the T^2 line is due to the T^4 term in Eq. (6).

B. Functions $b_1(V)$ and $c_1(V)$

The coefficients b_1 and c_1 are functions of voltage and arise from the WKB approximation. The specific volt-current characteristic for a given barrier potential $\varphi(x,V)$ can be given from Eq. (1) by evaluating b_1 and c_1 as functions of V. Stratton[8] has developed Eq. (1) further for small applied voltages, while maintaining an arbitrary barrier shape, by expanding b_1 and c_1 as the following quadratic power series in qV

$$b_1=b_{10}-b_{11}(qV)+b_{12}(qV)^2, \tag{7}$$

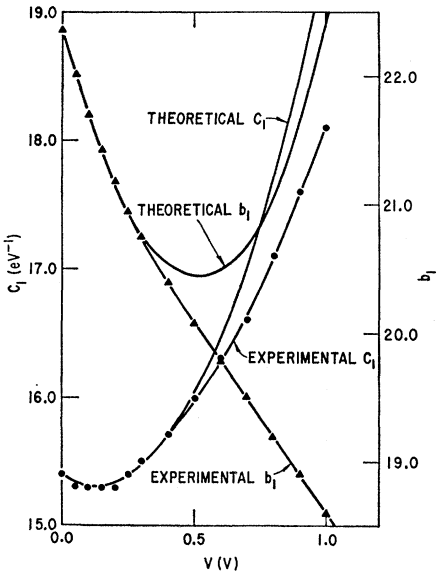

FIG. 6. The dependence of the coefficients b_1 and c_1 on voltage. The points are deduced from the experimental data by fitting the temperature dependence. The theoretical curves are quadratic power-series expansions corresponding to Eqs. (7) and (8).

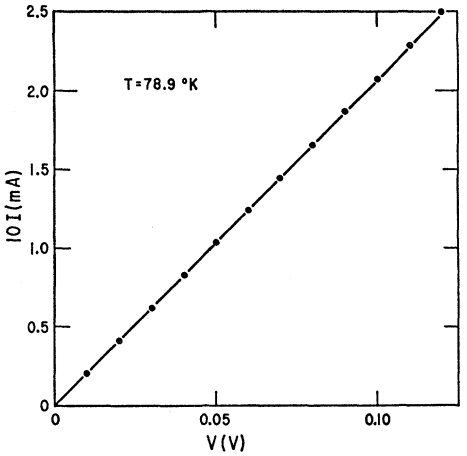

FIG. 7. Low-voltage Ohmic region. The current as a function of small applied voltage at $T=78.9$°K.

and

$$c_1=c_{10}-c_{11}(qV)+c_{12}(qV)^2. \tag{8}$$

By fitting the experimental current density data to the theoretical temperature dependence for a set of applied voltages in the range $0\leq V\leq 1.0$ V, b_1 and c_1 can be deduced as functions of V. The results are shown in Fig. 6. The experimental curves are plots of b_1 and c_1 deduced from the experimental data. The theoretical curves are the quadratic power-series expansions given in Eqs. (7) and (8) which have been fitted to the experimental curves for small applied voltages. The coefficients for the power series are listed in Table II. The region of applied voltage for which the quadratic power-series expansions in V, of the integrals arising from the WKB approximation, are valid, is seen to be $0.0\leq V\leq 0.3$ V.

Although c_1 can be represented approximately by the low-voltage quadratic over a substantially larger range of applied voltage, b_1 cannot. A plot of the current density as a function of voltage [cf. Fig. 2(a)] suggests a nearly linear approximation for b_1 in the range $0.2<V<1.0$ V, preceded by an Ohmic region (cf. Fig. 7). Stratton,[8] in analyzing the earlier data of Fischer and Giaever[27] and Pimbley,[28] fitted the quadratic power series for b_1 out to about 1.4 V. This procedure is equivalent essentially to fitting a parabola to the lower part of the experimental curve for b_1 shown in Fig. 6, which does not converge to the experimental curve for b_1 for

TABLE II. Quadratic power-series coefficients.

b_1	c_1 (eV)$^{-1}$
$b_{10}=22.37$	$c_{10}=15.38$ (eV)$^{-1}$
$b_{11}=7.56$ (eV)$^{-1}$	$c_{11}=1.32$ (eV)$^{-2}$
$b_{12}=7.4$ (eV)$^{-2}$	$c_{12}=5.29$ (eV)$^{-3}$

[27] J. C. Fisher and I. Giaever, J. Appl. Phys. 32, 172 (1961).
[28] W. T. Pimbley (unpublished).

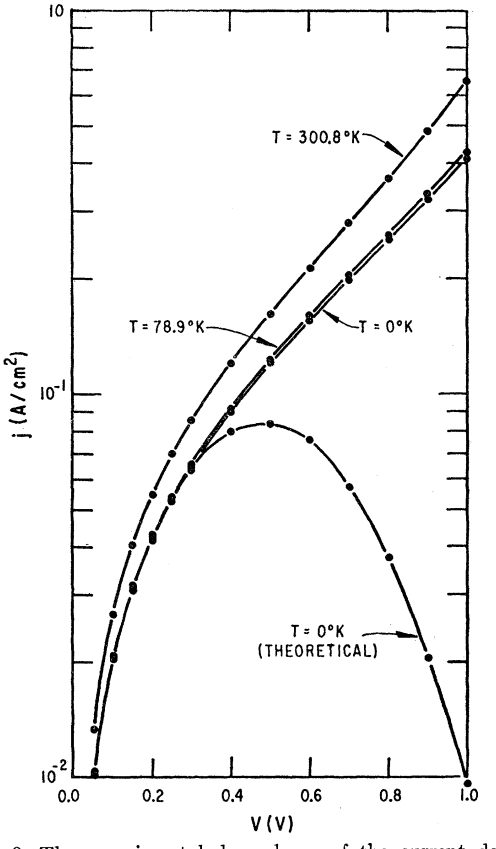

FIG. 8. The experimental dependence of the current density on the voltage at room, liquid nitrogen and extrapolated to absolute zero temperature. The theoretical curve was calculated, assuming the quadratic power-series approximations for b_1 and c_1, using Eq. (1).

small V. The coefficients of the quadratic expansions are related to physical properties of the potential barrier.[8] The numerical values for the physical properties reported by Stratton, therefore, are in error.

The low-voltage quadratic expansions given in Eqs. (7) and (8) using the coefficients in Table II were used to calculate the theoretical volt-current characteristic for $T=0°$K shown in Fig. 8. The experimental characteristics for room, liquid nitrogen and extrapolated to absolute zero temperature are also shown. It is apparent that the theoretical curve is a good representation for $0\leq V\leq 0.3$ V, which is the range of voltage for which the quadratic power-series expansion for b_1 is valid, and that the divergence between the theoretical and experimental curve for $T=0°$K results from the functional form of b_1 shown in Fig. 6.

The functional form of b_1 and c_1 shown in Fig. 6 for $V>0.3$ V is not expected to be universal. In particular, the functional form shown here pertains to an oxide grown by the technique described in Sec. IIA.

C. Physical Properties of the Barrier Layer

The numerical values of the coefficients in Table II can be related to the physical properties of the barrier when a particular barrier shape is assumed. Using Simmons' expression for the tunnel path length given in Eq. (4), b_1 and c_1 given by Eqs. (7) and (8), and the coefficients from Table II, it is easy to show that Δx is approximately constant over the range $0.2<V<0.6$ V which is consistent with a trapezoidal (or rectangular) barrier shape.

Using the asymmetry in the experimental current density with respect to the polarity of the applied potential, and the relation for asymmetrical barriers that[8]

$$b_{11}+b_{21}=c_{10}$$

a value of $b_{21}=7.82$ (eV)$^{-1}$ is obtained.

Assuming a trapezoidal barrier shape for $\varphi(x,V)$, integrating, carrying out the Taylor expansions with respect to energy and the binomial expansion in Eq. (7) (and assuming a corresponding series for b_2) leads to the following relationships between the physical parameters and the coefficients:

$$\left.\begin{aligned} b_{10}&=\frac{2\alpha L}{3}\left(\frac{\chi_2'^{3/2}-\chi_1'^{3/2}}{\chi_2'-\chi_1'}\right),\\ b_{11}&=(\alpha L\chi_2'^{1/2}-b_{10})/(\chi_2'-\chi_1'),\\ b_{21}&=-(\alpha L\chi_1'^{1/2}-b_{10})/(\chi_2'-\chi_1'),\end{aligned}\right\} \tag{9}$$

where

$$\chi_n=\chi_n'+\Delta\chi;\ n=1,2. \tag{10}$$

χ_1' and χ_2' are the effective heights of the trapezoidal barrier above the Fermi level on the side adjacent to metal 1 and 2, respectively, which differ from the true metal-insulator work functions χ_1 and χ_2 by an amount $\Delta\chi$. It will be assumed that the barrier is a result of two unequal metal-insulator work functions and the image force. In Simmons'[29] evaluation of b in terms of an average barrier height and an effective tunnel path, the image force barrier essentially is replaced by a rectangular barrier which is lower in height than the image force barrier by [cf. Simmons'[29] Eqs. (33) and (40)]

$$\Delta\chi=[1.15\lambda L/(x_2-x_1)]\ \ln[x_2(L-x_1)/x_1(L-x_2)] \tag{11}$$

for zero applied voltage, where

$$\lambda=(q^2/8\pi\kappa L)\ \ln 2,$$

and L is the thickness of the insulating film. The quantity $\Delta\chi=0.11$ eV for the parameters deduced from the experimental data. Using this value of $\Delta\chi$ as an approximate correction term in Eq. (10), solving Eqs. (9) simultaneously and substituting the values for b_{10}, b_{11}, and b_{21} yields

$$\chi_1=0.78\text{ eV};\ \chi_2=0.89\text{ eV}$$

which will represent a slight underestimate, and

$$L=25.7\text{ Å}$$

[29] J. G. Simmons, J. Appl. Phys. 34, 2581 (1963).

assuming an effective electron mass in the insulator $m^*/m=1$. Meyerhoffer and Ochs[17] have pointed out that the effective mass theoretically should be near to one.[30,31] Assuming a dielectric constant of 8.0,[18] the thickness of the insulating layer calculated from capacitance is 25.7 Å, and the tunnel path length, calculated from Eq. (4), is 25.6 Å. The aluminum film corresponding to χ_1 is the one on which the oxide was grown. Greater currents are passed when this layer is positive, which is in agreement with other observations.[15,17]

A plot of the experimental data for a thicker aluminum oxide (formed in an oxygen glow discharge) and larger applied voltages is shown in Fig. 9. The data are plotted as $\log I/V^2$ versus $1/V$ for comparison with the Fowler-Nordheim theory.[2] Including the image force correction the slope (for large V) results in a value of $\chi_2=0.85$ eV, which is in good agreement with the value deduced from the low-voltage measurements.

[*Note added in proof.* Recent investigations on the thicker aluminum oxides at larger applied voltages (similar to specimens used to obtain the data shown in Fig. 9) indicate considerably larger effective barrier heights and smaller effective thicknesses than are obtained from the analysis of low-voltage data. The barrier heights given above are based on the assumption of a trapezoidal barrier shape which does not appear to be an adequate representation for all voltages.]

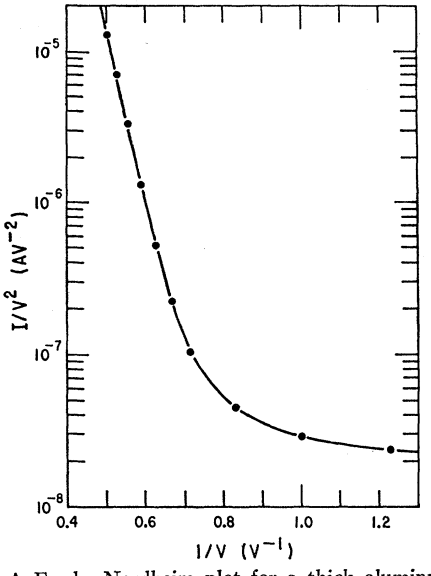

FIG. 9. A Fowler-Nordheim plot for a thick aluminum oxide film. The slope leads to an approximate metal-insulator work function of $\chi_2=0.85$ eV.

[30] E. O. Kane, Phys. Chem. Solids 1, 245 (1957).
[31] R. Braunstein and E. O. Kane, Phys. Chem. Solids 23, 1423 (1962).

V. CONCLUSIONS

The current density through aluminum oxide films less than 30 Å thick, sandwiched between two aluminum films, is presented as a function of temperature and voltage. The analysis of the temperature dependence of the data established that tunneling directly between the two aluminum layers is the predominant mechanism for electron conduction through the aluminum oxide film.

The data are analyzed using the theory of Stratton. The theory is modified to take more accurate account of the back current and compared with the theory of Simmons. Both the modified and Simmons expressions are intractable to experimental analysis. It is indicated that the errors involved in using the simplified version of Stratton's theory are small, therefore, the original form given in Eq. (1), is employed.

The region of validity is established, for quadratic power-series expansions in V, of the integrals arising from the WKB approximation. Fitting the quadratics to the experimental curves for these integrals results in approximate values for the heights of the potential barrier above the Fermi level and the barrier thickness, when a trapezoidal barrier shape (modified by image forces) is assumed.

The actual shape of the potential barrier cannot be extracted with any degree of confidence using only the low-voltage current-density data as a function of temperature. Therefore, even though the preliminary Fowler-Nordheim analysis results in a barrier height in agreement with the value obtained for an image force barrier, a more elaborate investigation is required.

ACKNOWLEDGMENTS

The authors acknowledge with thanks the many helpful and stimulating discussions with R. Stratton and N. G. Einspruch, the technical assistance of P. J. May, Jr., J. W. Taylor for the preparation of samples, and J. C. Blair for the data shown in Fig. 9.